ELECTROMAGNETIC POLARIZATION IN PARTIALLY IONIZED PLASMAS WITH STRONG MAGNETIC FIELDS AND NEUTRON STAR ATMOSPHERE MODELS

Alexander Y. Potekhin,[1,2] Dong Lai,[3] Gilles Chabrier,[4] and Wynn C. G. Ho[5,6]
Draft version February 2, 2008

ABSTRACT

Polarizability tensor of a strongly magnetized plasma and the polarization vectors and opacities of normal electromagnetic waves are studied for the conditions typical of neutron star atmospheres, taking account of partial ionization effects. Vacuum polarization is also included using a new set of fitting formulae that are accurate for wide range of field strengths. The full account of the coupling of the quantum mechanical structure of the atoms to their center-of-mass motion across the magnetic field is shown to be crucial for the correct evaluation of the polarization properties and opacities of the plasma. The self-consistent treatment of the polarizability and absorption coefficients proves to be necessary if the ionization degree of the plasma is low, which can occur in the atmospheres of cool or ultramagnetized neutron stars. Atmosphere models and spectra are presented to illustrate the importance of such self-consistent treatment.

Subject headings: magnetic fields—plasmas—stars: atmospheres—stars: neutron—X-rays: stars

1. INTRODUCTION

In recent years, thermal or thermal-like radiation has been detected from several classes of isolated neutron stars (NSs): radio pulsars with typical magnetic fields $B \sim 10^{12}$–10^{13} G, "dim" NSs whose magnetic fields are mostly unknown, anomalous X-ray pulsars and soft gamma-ray repeaters with B possibly $\sim 10^{14}$–10^{15} G (see, e.g., Becker & Aschenbach 2002; Haberl 2004; Israel, Mereghetti, & Stella 2002; Pavlov & Zavlin 2003, for reviews). The spectrum of thermal radiation is formed in a thin atmospheric layer (with scale height ~ 0.1–10 cm and density $\rho \sim 10^{-2}$–10^3 g cm^{-3}) that covers the stellar surface. Therefore, a proper interpretation of the observations of NS surface emission requires understanding of radiative properties of these magnetized atmospheres.

Shibanov et al. (1992) (see also Shibanov & Zavlin 1995; Pavlov et al. 1995) presented the first model of the NS atmospheres with strong magnetic fields, assuming full ionization. Variants of this model were constructed by Zane, Turolla, & Treves (2000); Zane et al. (2001); Ho & Lai (2001, 2003); Özel (2001); Lloyd (2003). An inaccurate treatment of the absorption due to free-free transitions in strong magnetic fields in the earlier models (Pavlov et al. 1995) has been corrected by Potekhin & Chabrier (2003); this correction has been taken into account in later models (Ho et al. 2003, 2004; Lloyd 2003). Recent work (Ho & Lai 2003; Lai & Ho 2002, 2003a) has shown that in the magnetar field regime

[1] Ioffe Physico-Technical Institute, Politekhnicheskaya 26, 194021 St. Petersburg, Russia; palex@astro.ioffe.ru
[2] Isaac Newton Institute of Chile, St. Petersburg Branch, Russia
[3] Center for Radiophysics and Space Research, Department of Astronomy, Cornell University, Ithaca, NY 14853; dong@astro.cornell.edu
[4] Ecole Normale Supérieure de Lyon (CRAL, UMR CNRS No. 5574), 46 allée d'Italie, 69364 Lyon Cedex 07, France; chabrier@ens-lyon.fr
[5] Kavli Institute for Particle Astrophysics and Cosmology, Stanford University, PO Box 20450, Mail Stop 29, Stanford, CA 94309; wynnho@slac.stanford.edu
[6] Hubble Fellow

($B \gtrsim 10^{14}$ G) vacuum polarization significantly affects the emergent spectrum from the atmosphere; for weaker fields, vacuum polarization can still leave an unique imprint on the X-ray polarization signals (Lai & Ho 2003b).

Because the strong magnetic field significantly increases the binding energies of atoms, molecules, and other bound states (see Lai 2001, for a review), these bound states may have abundances appreciable enough to contribute to the opacity in the atmosphere. For calculation of this contribution, the non-trivial coupling of the center-of-mass (CM) motion of the atom to its internal structure (e.g., Potekhin 1994, and references therein) can be important. Also, because of the relatively high atmosphere density, a proper treatment should take account of the plasma nonideality that leads to Stark broadening and pressure ionization. Recently, thermodynamically consistent equation of state (EOS) and opacities have been obtained for a magnetized, partially ionized H plasma for 8×10^{11} G $\lesssim B \leq 10^{15}$ G (Potekhin, Chabrier, & Shibanov 1999; Potekhin & Chabrier 2003, 2004). These EOS and opacities have been implemented by Ho et al. (2003, 2004) for modeling NS atmospheres. For the typical field strengths $B = 10^{12}$–10^{13} G this modeling showed that, although the spectral features due to neutral atoms lie at extreme UV and very soft X-ray energy bands and therefore are difficult to observe, the continuum flux is also different from the fully ionized case, especially at lower energies, which can affect fitting of the observed spectra. For the superstrong field $B \gtrsim 10^{14}$ G, Ho et al. (2003) showed that the vacuum polarization effect not only suppresses the proton cyclotron line, but also suppresses spectral features due to bound species.

It is well known (e.g., Ginzburg 1970; Mészáros 1992) that under typical conditions (e.g., far from the resonances) radiation propagates in a magnetized plasma in the form of two so-called extraordinary and ordinary normal modes. The polarization vectors of these modes, $\boldsymbol{e}^{\mathrm{X}}$ and $\boldsymbol{e}^{\mathrm{O}}$ are determined by the Hermitian part ($\boldsymbol{\chi}^{\mathrm{H}}$) of the complex polarizability tensor ($\boldsymbol{\chi}$) of the plasma. Our previous treatment of these modes in partially ionized

atmospheres (Potekhin & Chabrier 2003, 2004; Ho et al. 2003, 2004) was not quite self-consistent, because the effect of the presence of the bound states on the polarization of normal modes was neglected: we adopted the same polarization vectors as in the fully ionized plasma, assuming (Potekhin & Chabrier 2003) that the effect of bound states on these vectors should be small provided the ionization degree of the plasma is high. However, this hypothesis (related to χ^{H}) may be called into question, based on the observation that the absorption coefficients (corresponding to the anti-Hermitian part of the complex polarizability tensor, $i\chi^{\mathrm{A}}$) are strikingly affected by the presence of even a few percent of the atoms.

In this paper, we study the polarizability tensor, the polarization vectors of the normal waves, and the opacities of the partially ionized nonideal hydrogen plasma in strong magnetic fields in a self-consistent manner, using the technique applied previously by Bulik & Pavlov (1996) to the case of a monatomic ideal hydrogen gas. In §2 we introduce basic definitions and formulae to be used for calculation of the plasma polarizability (new fitting formulae for the vacuum polarizability are given in the Appendix). An approximate model based on a perturbation theory, which explains the importance of the CM coupling for plasma polarizability, is described in §3. The results of numerical calculations of the plasma polarizability are presented in §4, and the consequences for the polarization and opacities of the normal modes are discussed in §5. In §6 we present examples of NS thermal spectra, calculated using the new opacities, compared with the earlier results. In §7 we summarize our results, outline the range of their applicability, and discuss unsolved problems.

2. GENERAL FORMULAE FOR POLARIZATION IN A MAGNETIZED PLASMA

2.1. Complex Polarizability Tensor

The propagation of electromagnetic waves in a medium is described by the wave equation that is obtained from the Maxwell equations involving the tensors of electric permittivity $\boldsymbol{\epsilon}$, magnetic permeability $\boldsymbol{\mu}$, and electrical conductivity $\boldsymbol{\sigma}$. It is convenient (e.g., Ginzburg 1970) to introduce the complex dielectric tensor $\boldsymbol{\epsilon}' = \boldsymbol{\epsilon} + 4\pi i\boldsymbol{\sigma}/\omega$. In the strong magnetic field, it should include the vacuum polarization. When the vacuum polarization is small, it can be linearly added to the plasma polarization. Then we can write

$$\boldsymbol{\epsilon}' = \mathbf{I} + 4\pi\boldsymbol{\chi} + 4\pi\boldsymbol{\chi}^{\mathrm{vac}}, \qquad (1)$$

where $\mathbf{I}$ is the unit tensor, $\boldsymbol{\chi} = \boldsymbol{\chi}^{\mathrm{H}} + i\boldsymbol{\chi}^{\mathrm{A}}$ is the complex polarizability tensor of the plasma, and $\boldsymbol{\chi}^{\mathrm{vac}}$ is the polarizability tensor of the vacuum.

In the Cartesian coordinate system $x'y'z'$ with unit vectors $\hat{\mathbf{x}}'$, $\hat{\mathbf{y}}'$, $\hat{\mathbf{z}}'$, where $\hat{\mathbf{z}}'$ is along magnetic field $\boldsymbol{B}$, the electric permittivity tensor of a plasma in the dipole approximation, the dielectric vacuum correction, and the inverse magnetic permeability of the vacuum can be written, respectively, as (e.g., Ho & Lai 2003, and references therein)

$$\mathbf{I} + 4\pi\boldsymbol{\chi} = \begin{bmatrix} \varepsilon & ig & 0 \\ -ig & \varepsilon & 0 \\ 0 & 0 & \eta \end{bmatrix}, \qquad (2)$$

$$4\pi\boldsymbol{\chi}^{\mathrm{vac}} = \mathrm{diag}(\hat{a}, \hat{a}, \hat{a} + q), \qquad (3)$$

$$\boldsymbol{\mu}^{-1} = \mathbf{I} + \mathrm{diag}(\hat{a}, \hat{a}, \hat{a} + m), \qquad (4)$$

where $\hat{a}$, q, and m are vacuum polarization coefficients which vanish at $B = 0$. The formulae for calculation of these coefficients are given in the Appendix. Quantities ε, η, and g are well known for fully ionized ideal plasmas (e.g., Ginzburg 1970). In this paper we shall calculate χ for partially ionized hydrogen plasmas at typical NS atmosphere conditions.

The complex polarizability tensor of a plasma becomes diagonal, $\boldsymbol{\chi} = \mathrm{diag}(\chi_{+1}, \chi_{-1}, \chi_0)$ in the cyclic or rotating coordinates, where the cyclic unit vectors are defined as $\hat{\mathbf{e}}_0 = \hat{\mathbf{z}}'$, $\hat{\mathbf{e}}_{\pm 1} = (\hat{\mathbf{x}}' \pm i\hat{\mathbf{y}}')/\sqrt{2}$. The real parts of the components χ_α $(\alpha = \pm 1, 0)$ determine the Hermitian tensor $\boldsymbol{\chi}^{\mathrm{H}}$, which describes the refraction and polarization of waves, and their imaginary parts determine the anti-Hermitian tensor $i\boldsymbol{\chi}^{\mathrm{A}}$, responsible for the absorption. According to equation (2),

$$4\pi\chi_{\pm 1} = \varepsilon - 1 \pm g, \quad 4\pi\chi_0 = \eta - 1. \qquad (5)$$

Note that in the cyclic representation, the general symmetry relations for the polarizability tensor take the form

$$\chi_\alpha^{\mathrm{A}}(-\omega) = -\chi_{-\alpha}^{\mathrm{A}}(\omega), \quad \chi_\alpha^{\mathrm{H}}(-\omega) = \chi_{-\alpha}^{\mathrm{H}}(\omega). \qquad (6)$$

2.2. Relation Between the Plasma Polarizability and Absorption

General expressions in the dipole approximation for χ_α^{A} and χ_α^{H} through frequencies and oscillator strengths of quantum transitions in a magnetized medium are given, e.g., by Bulik & Pavlov (1996). For transitions between two stationary quantum states i and f with energies E_i and $E_f = E_i + \hbar\omega_{fi} > E_i$ and number densities of the occupied states n_i and n_f, the absorption coefficient for the basic polarization α equals (see, e.g., Armstrong & Nicholls 1972)

$$\mu_\alpha^{if} \equiv \rho\hat{\kappa}_\alpha(\omega) = \frac{2\pi^2 e^2}{m_e c} (n_i - n_f) f_\alpha^{if} \delta(\omega - \omega_{fi}), \qquad (7)$$

where $f_\alpha^{if} = (2m_e\omega_{fi}/\hbar) |\langle f|\boldsymbol{r}|i\rangle \cdot \hat{\mathbf{e}}_\alpha|^2$ is the oscillator strength for the transition $i \to f$. These partial absorption coefficients sum up into the total $\mu_\alpha = \sum_{i,f(E_f>E_i)} \mu_\alpha^{if}$, where $\sum_{i,f}$ includes integration over continuum states. Then the equation

$$\chi_\alpha^{\mathrm{A}}(\omega) = \frac{c}{4\pi\omega} \mu_\alpha(\omega), \qquad (8)$$

together with the first symmetry relation (6) yield

$$\chi_\alpha^{\mathrm{A}}(\omega) = \frac{\pi e^2}{2m_e\omega} \sum_{i,f(E_f>E_i)} (n_i - n_f) \\ \times \left[f_\alpha^{if} \delta(\omega - \omega_{fi}) + f_{-\alpha}^{if} \delta(\omega + \omega_{fi}) \right]. \qquad (9)$$

Once χ^{A} is known, χ^{H} can be calculated from the Kramers-Kronig relation (Landau & Lifshitz 1989, §123) or its modification (Bulik & Pavlov 1996),

$$\chi_\alpha^{\mathrm{H}}(\omega) = \frac{1}{\pi\omega} \mathcal{P} \int_{-\infty}^{\infty} \frac{\omega'\chi_\alpha^{\mathrm{A}}(\omega')}{\omega' - \omega} \, d\omega', \qquad (10)$$

where $\mathcal{P}\int$ means the principal value of the integral. From equations (9) and (10),

$$\chi_\alpha^{\mathrm{H}}(\omega) = -\frac{e^2}{2m_e\omega} \sum_{i,f(E_f>E_i)} (n_i - n_f) \left[\frac{f_\alpha^{if}}{\omega - \omega_{fi}} + \frac{f_{-\alpha}^{if}}{\omega + \omega_{fi}} \right]. \qquad (11)$$

Taking into account equations (8) and (6), we can present relation (10) in the form convenient for calculation at $\omega > 0$:

$$\chi_\alpha^{\mathrm{H}}(\omega) = \frac{c}{4\pi^2\omega}\left\{\int_0^\omega \left[\mu_\alpha(\omega+\omega') - \mu_\alpha(\omega-\omega')\right]\frac{\mathrm{d}\omega'}{\omega'} \right.$$
$$\left. + \int_{2\omega}^\infty \frac{\mu_\alpha(\omega')}{\omega'-\omega}\,\mathrm{d}\omega' - \int_0^\infty \frac{\mu_{-\alpha}(\omega')}{\omega'+\omega}\,\mathrm{d}\omega'\right\}. \quad (12)$$

If we replace delta-function in equation (7) by the Lorentz profile $(\nu_\alpha^{if}/\pi)\left[(\omega-\omega_\alpha)^2 + (\nu_\alpha^{if})^2\right]^{-1}$, where ν_α^{if} is a damping rate for a given transition, then equations (9) and (11) can be combined to give

$$\chi_\alpha(\omega) = -\frac{e^2}{2m_e\omega}\sum_{i,f\,(E_f>E_i)}(n_i-n_f)\left[\frac{f_\alpha^{if}}{\omega-\omega_{fi}+i\nu_\alpha^{if}}\right.$$
$$\left. + \frac{f_{-\alpha}^{if}}{\omega+\omega_{fi}+i\nu_{-\alpha}^{if}}\right]. \quad (13)$$

3. ANALYTIC MODEL OF POLARIZATION OF ATOMIC GAS: EFFECT OF CENTER-OF-MASS MOTION

As mentioned in §1, in strong magnetic fields the internal structure of an atom is strongly coupled to its CM motion perpendicular to the field. This coupling (referred to as "CM coupling") has a significant effect on the radiative opacities and dielectric property of the medium. Before presenting numerical results for the polarizability tensor of a partially ionized plasma in §4, it is useful to consider an analytic model to illustrate this CM coupling effect.

Consider an atomic gas in which the atom possesses only two energy levels, with the upper level having the radiative (Lorentz) width ν, assumed to be constant for simplicity. The energies of the (moving) atom in the ground state and the excited state are denoted by $E_1(\boldsymbol{P})$ and $E_2(\boldsymbol{P}')$ respectively, where $\boldsymbol{P}$ and $\boldsymbol{P}'$ are the CM pseudo-momenta, and the subscripts 1 and 2 specify the internal degree of freedom of the atom. [In strong magnetic fields, the internal quantum numbers are (s,ν_z), where $s = 0,1,2,\cdots$ measures the relative angular momentum between the proton and electron, and ν_z is related to the number of nodes in the z direction.] If there were no CM coupling, we would have $E_{1,2}(\boldsymbol{P}) = E_{1,2}(0) + \boldsymbol{P}^2/(2m_{\mathrm{H}})$ and $\omega_{21} \equiv (E_2-E_1)/\hbar$ =constant. Therefore, in this case equation (13) would yield

$$\chi_\alpha(\omega) \simeq -\frac{e^2 n_1}{2m_e\omega}\left[\frac{f_\alpha^{12}}{\omega-\omega_{21}+i\nu} + \frac{f_{-\alpha}^{12}}{\omega+\omega_{21}+i\nu}\right]. \quad (14)$$

This would imply that even for very small neutral atom fraction, the bound-bound transition can severely affect the dielectric property of the gas in the neighborhood of $\omega = \omega_{21}$ (for $\nu \ll \omega_{21}$).

However, in strong magnetic fields, the energy associated with the transverse CM motion of the atom cannot be separated from the internal energy. We therefore have

$$\chi_\alpha(\omega) = -\frac{e^2 n_1}{2m_e\omega}\int \frac{p_1(P_\perp)\,\mathrm{d}^2 P_\perp}{(2\pi\hbar)^2}\left[\frac{f_\alpha^{12}(\boldsymbol{P}_\perp)}{\omega-\omega_{21}(P_\perp)+i\nu}\right.$$
$$\left. + \frac{f_{-\alpha}^{12}(\boldsymbol{P}_\perp)}{\omega+\omega_{21}(P_\perp)+i\nu}\right], \quad (15)$$

where $\boldsymbol{P}_\perp$ is the transverse pseudo-momentum, $p_1(P_\perp)\,\mathrm{d}^2 P_\perp$ is the probability to find an atom in the initial state "1" in an element $\mathrm{d}^2 P_\perp$ near $\boldsymbol{P}_\perp$ (see Potekhin et al. 1999), and we have used the fact that the oscillator strength is nonzero only when $\boldsymbol{P} = \boldsymbol{P}'$ (in the dipole approximation). The CM coupling effect will significantly smooth out the divergent behavior at $\omega = \omega_{21}$ in equation (14) (for $\nu \to 0$). This effect can be taken into account using the perturbation result of Pavlov & Mészáros (1993), as was done by Bulik & Pavlov (1996), or numerically, using the techniques of Pavlov & Potekhin (1995) and Potekhin & Pavlov (1997).

In the perturbation theory, valid for small $P_\perp$, the coupling reveals itself as an effective "transverse" mass $M_\perp > m_{\mathrm{H}}$ acquired by the atom, which is different for different quantum levels. For the two-level atom, the perturbation theory gives $E_j(P_\perp) = E_j(0) + P_\perp^2/(2M_{\perp j})$ $(j = 1,2)$, and we find

$$\chi_\alpha \simeq -\frac{e^2 n_1}{2m_e\omega}\int_0^\infty \mathrm{d}y\left[\frac{f_\alpha^{12}\,e^{-y}}{\omega-\omega_{21}(0)+i\nu+a(T)\,y}\right.$$
$$\left. + \frac{f_{-\alpha}^{12}\,e^{-y}}{\omega+\omega_{21}(0)+i\nu+a(T)\,y}\right], \quad (16)$$

where $a(T) = (k_{\mathrm{B}}T/\hbar)(1-M_{\perp 1}/M_{\perp 2})$, and we have used $p_1(P_\perp) \propto \exp[-P_\perp^2/(2M_{\perp 1}k_{\mathrm{B}}T)]$. At $\nu \to 0$, only weak logarithmic divergence is present near $\omega = \omega_{21}$, compared to the much stronger $(\omega-\omega_{21})^{-1}$ divergence in equation (14). Additional line broadening due to collisions (which implies $\nu \neq 0$), thermal effect and pressure effect, not treated in this simple model, will further smooth out the "divergent" feature in the polarizability tensor.

This simple model shows that a proper treatment of the CM coupling is important in calculating the polarizability tensor of a partially ionized plasma. In practice, since the absorption coefficient μ_α has already been calculated by Potekhin & Chabrier (2003, 2004), we find it is more convenient to apply the Kramers-Kronig transformation (eq. [12]) to obtain χ_α^{H} (see §4).

4. EFFECT OF PARTIAL IONIZATION ON POLARIZABILITY OF A STRONGLY MAGNETIZED HYDROGEN PLASMA

Some approximations for calculation of the complex dielectric tensor of a plasma have been discussed, for example, by Ginzburg (1970). In particular, the "elementary theory" gives the expression widely used in the past to describe polarization properties of the fully ionized electron-ion plasma (e.g., Shibanov et al. 1992; Zane et al. 2000; Ho & Lai 2001, 2003):

$$4\pi\chi_\alpha = -\frac{\omega_{\mathrm{pl}}^2}{(\omega+\alpha\omega_{ce})(\omega-\alpha\omega_{ci})+i\omega\nu_{\mathrm{eff}}}, \quad (17)$$

where $\omega_{ce} = eB/m_e c$ and $\omega_{ci} = ZeB/m_i c$ are the electron and ion cyclotron frequencies, $\omega_{\mathrm{pl}} = (4\pi n_e e^2/m_e)^{1/2}$ is the electron plasma frequency, ν_{eff} is the effective damping frequency, m_i is the ion mass, Ze is the ion charge, and n_e is the electron number density. For the hydrogen plasma, the corresponding energies are $\hbar\omega_{ce} = 11.577\,B_{12}$ keV, $\hbar\omega_{ci} = 6.3049\,B_{12}$ eV, where $B_{12} = B/10^{12}$ G, and $\hbar\omega_{\mathrm{pl}} = 0.0287\sqrt{\rho}$ keV, where ρ is in g cm^{-3}. In general, the damping frequency ν_{eff}
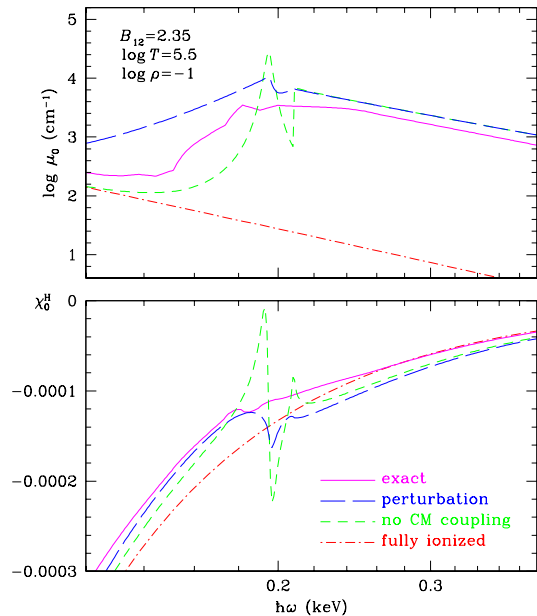
FIG. 1.— Absorption coefficient (upper panel) and polarizability (lower panel) of a hydrogen plasma for longitudinal polarization ($\alpha = 0$) at $B = 2.35 \times 10^{12}$ G, $\rho = 0.1$ g cm^{-3}, and $T = 3.16 \times 10^5$ K, according to four different models: fully ionized plasma (dot-dashed lines), partially ionized plasma without the effect of coupling between CM motion and internal structure of the atom (short dashes), with the magnetic broadening taken into account by perturbation theory (long dashes) and numerical calculation beyond the perturbation approximation (solid lines).

FIG. 2.— Same as in Figure 1, but for $\alpha = +1$.

depends on polarization and photon frequency. Derivation of equation (17) is based on the assumption that the electrons and ions lose their ordered velocities (imparted by the electric field of the electromagnetic wave) at the rate ν_{eff} which does not depend on the velocity. A more rigorous kinetic theory gives χ_α^A and χ_α^H which cannot be in general described by equation (17) using the same ν_{eff} (e.g., Ginzburg 1970, §6). For instance, if we describe χ_α^A using equation (17) with some frequency-dependent $\nu_{\text{eff}}(\omega)$, then the Kramers-Kronig transformation will give χ_α^H which, in general, does not coincide with the real part of equation (17) with the same $\nu_{\text{eff}}(\omega)$, although, for realistic $\nu_{\text{eff}}(\omega)$, the difference should be small at $\omega \gg \omega_{\text{pl}}$.

Realistic models of the absorption coefficients of a partially ionized plasma do not allow us to perform the Kramers-Kronig transformation analytically. We evaluated the integrals in equation (12) numerically. Since the integrand can be sharply peaked near resonance frequencies, we employed the adaptive-stepsize Runge-Kutta integration (Press et al. 1996, §16.2). The accuracy of the numerical transformation was tested with the models that allow one to perform the Kramers-Kronig transformation analytically – those given by equations (14) and (17) above, and by equations (49)–(53) of Bulik & Pavlov (1996) – and proved to be within 0.1%.

Let us first consider a model that neglects the CM coupling and the plasma nonideality. The absorption coefficient of the fully ionized component of the plasma includes contributions due to the free-free absorption and scattering on free electrons an protons. For the atoms,
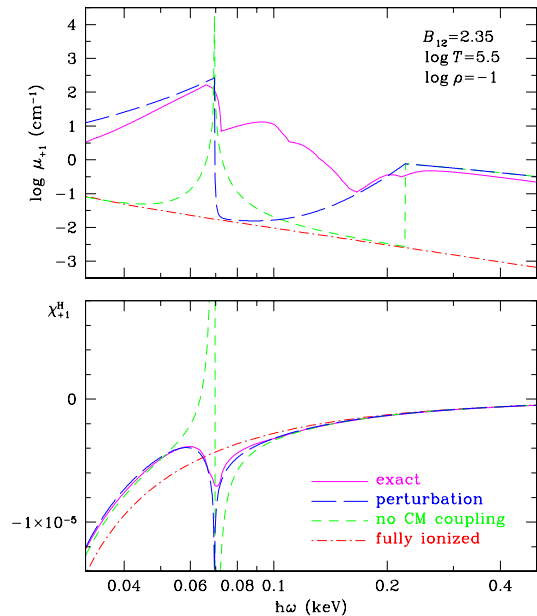
we include in consideration the bound-bound transition with the largest oscillator strength (for every polarization) and the bound-free transitions. In this case the absorption by the atom can be described by analytic formulae. The bound-bound absorption cross section is described by the Lorentz profile, where the effective damping width is mainly contributed by the electron impact broadening (Pavlov & Potekhin 1995) and can be evaluated using a fitting formula (Potekhin 1998). The bound-free cross sections are well described in the adiabatic approximation (however this is not true with the CM coupling, see Potekhin & Pavlov 1997); they are reproduced by fitting formulae in Potekhin & Pavlov (1993). For $B = 2.35 \times 10^{12}$ G, $\rho = 0.1$ g cm^{-3}, $T = 10^{5.5}$ K (the neutral fraction $x_{\text{H}} \approx 0.12$), the resulting absorption coefficients are shown by the short-dashed lines in Figures 1 and 2 for $\alpha = 0$ and $+1$, respectively. For $\alpha = 0$ this absorption profile is similar to the idealized model considered above. The corresponding $\chi_\alpha^H(\omega)$ are shown by the short-dashed lines on the lower panels of Figures 1 and 2. In each figure, dot-dashed lines correspond to the model of a fully ionized hydrogen plasma at the same B, ρ, and T. As in the above analytic model, we see that the presence of the atoms results in strong deviation from the fully ionized plasma model in the vicinity of the principal atomic resonances (the bound-free resonance for $\alpha = +1$ is almost invisible on the lower panel of Fig. 2 because of its small oscillator strength).

The absorption coefficients obtained using the perturbation theory of magnetic broadening (§3) are shown by the long-dashed lines on the upper panels of Figures 1 and 2. The long-dashed lines on the lower panels show the corresponding polarizabilities. We see that the resonant features are smoothed down by the magnetic broadening, and the resulting curves of $\chi_\alpha^H(\omega)$ do not much differ from the fully ionized plasma model.
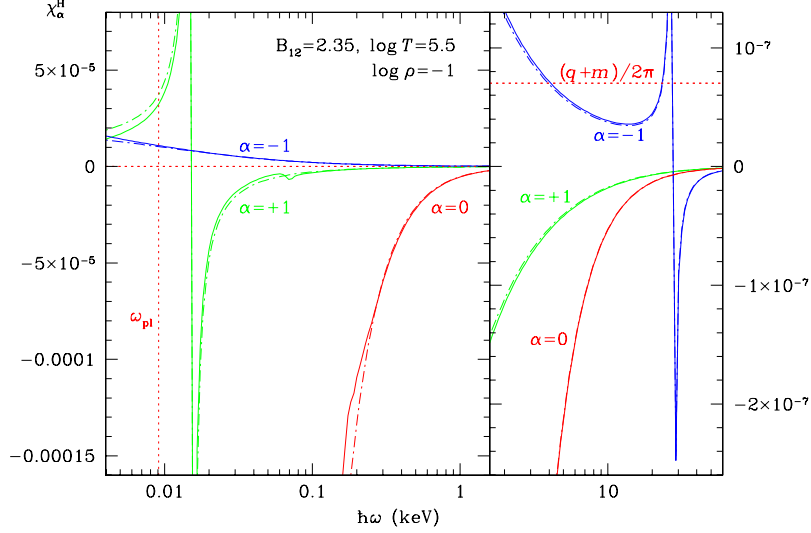
Still greater smoothing occurs for the accurate (non-

FIG. 3.— Polarizabilities χ_α^H ($\alpha = \pm 1, 0$) of the partially ionized (solid lines) and fully ionized (dot-dashed lines) plasma with the same parameters as in Figures 1, 2. The right part of the figure has an enlarged vertical scale. The dotted lines correspond to $\omega_{\rm pl}$ (vertical) and $(q + m)/(2\pi)$ (horizontal), where q and m are the vacuum polarization parameters.

perturbative) functions $\mu_\alpha(\omega)$ and $\chi_\alpha^H(\omega)$ (solid lines in the figures). The absorption coefficients shown on the upper panels correspond to the opacities in Figure 9 of Potekhin & Chabrier (2003). The significant difference of these absorption coefficients from the perturbational ones arises partly from the dependence of the oscillator strengths on the atomic velocity across the field, partly from transitions which were dipole-forbidden for the atom at rest and were not taken into account in the perturbation approximation described above, and partly from the nonideal plasma effect of continuum lowering. Nevertheless, despite these differences in μ_α, the difference in χ_α^H is much less significant.

Figure 3 shows all three components χ_α^H in a wider energy range. In this figure, as well as in the previous two, the polarizabilities in the fully ionized plasma model, shown by the dot-dashed lines, are obtained from equation (12), where the free-free contribution to $\mu_\alpha(\omega)$ includes the frequency-dependent Coulomb logarithm $\Lambda_\alpha^{\rm ff}$ (Potekhin & Chabrier 2003). Because of this frequency dependence, these polarizabilities are not identical to the ones given by equation (17), the difference being small at $\omega \gg \omega_{\rm pl}$ and appreciable at $\omega \lesssim \omega_{\rm pl}$, where both the elementary theory and the description of absorption by binary collisions (i.e., neglecting the collective motion effects) are rather inaccurate. The solid lines, which are obtained for the partially ionized plasma, are fairly close to the dot-dashed lines. The only prominent features are the proton and electron cyclotron resonances at $\hbar\omega_{\rm ci} = 0.0148$ keV and $\hbar\omega_{\rm ce} = 27.21$ keV.

However, such smoothing does not always occur. Let us consider a higher magnetic field $B = 3 \times 10^{13}$ G and density $\rho = 1$ g cm^{-3}, retaining the same temperature. Then $x_{\rm H} = 0.89$. Figure 4 demonstrates the absorption coefficients and polarizabilities for the fully ionized (dot-dashed lines) and partially ionized (solid lines) plasma. In addition to the proton cyclotron resonance at $\hbar\omega = 0.19$ keV, absorption coefficients in the partially ionized plasma exhibit magnetically broadened bound-

bound and bound-free features. The most prominent are the bound-bound absorption at $\hbar\omega \approx 0.2$–0.3 keV for μ_{+1} and the photoionization edge at $\hbar\omega = 0.408$ keV for μ_0. These features are clearly reflected in the behavior of χ_{+1}^H and χ_0^H, shown in the lower panels. Thus, with increasing B, the abundance of neutral states increases along with their influence on the polarizability.

A similar trend occurs with lowering T. If, for example, in the previous case ($B = 2.35 \times 10^{12}$ G, $\rho = 0.1$ g cm^{-3}) we take a lower $T = 1.58 \times 10^5$ K, then we will have 94.1% of H atoms in the ground state, 1.3% in the excited states, and 1.1% of H$_2$ molecules. At $\rho = 1$ g cm^{-3}, the abundance of the atoms will be 96.9% (with roughly equal fractions of excited states and molecules), and we nearly recover the case studied by Bulik & Pavlov (1996), who assumed 100% of atoms for these plasma parameters.

5. EFFECT OF PARTIAL IONIZATION ON POLARIZATION AND OPACITIES OF NORMAL MODES

In the coordinate system xyz with z along the wave vector of the photon and $\boldsymbol{B}$ in the x–z plane, the polarization vectors $\boldsymbol{e}^j$ of the normal modes in a magnetized plasma can be written as (Ho & Lai 2003)

$$(e_x^j, e_y^j, e_z^j) = (1 + K_j^2 + K_{z,j}^2)^{-1/2}\,(iK_j, 1, iK_{z,j}), \quad (18)$$

where $j = 1, 2$ correspond to the extraordinary mode (X-mode) and ordinary mode (O-mode). The parameters K_j and $K_{z,j}$ are expressed in terms of the components of the dielectric and magnetic tensors as

$$K_j = \beta\left\{ 1 + (-1)^j \left[1 + \frac{1}{\beta^2} + \frac{m}{1+\hat{a}}\frac{\sin^2\theta_B}{\beta^2} \right]^{1/2} \right\}, \quad (19)$$

$$K_{z,j} = -\frac{(\varepsilon' - \eta')K_j\cos\theta_B + g}{\varepsilon'\sin^2\theta_B + \eta'\cos^2\theta_B}\sin\theta_B, \quad (20)$$

where

$$\beta = \frac{\eta' - \varepsilon' + g^2/\varepsilon' + \eta'\, m/(1+\hat{a})}{2\,g}\frac{\varepsilon'}{\eta'}\frac{\sin^2\theta_B}{\cos\theta_B}, \quad (21)$$
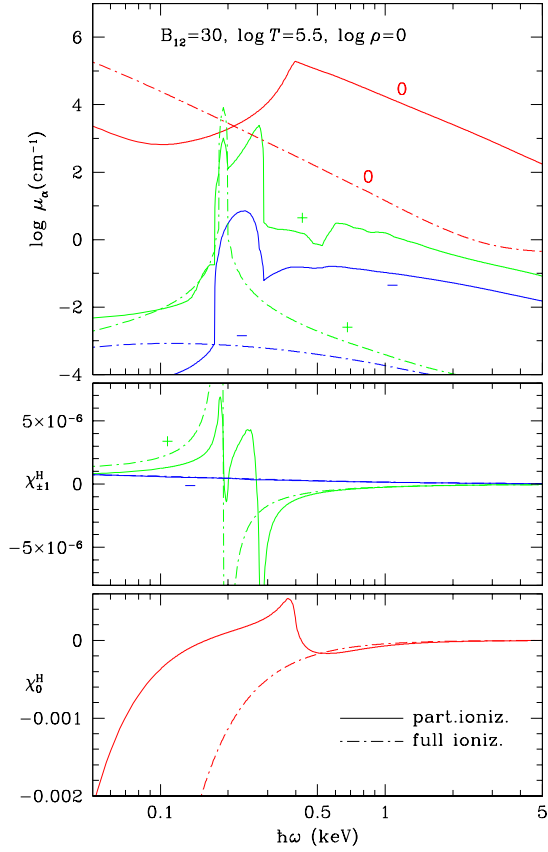
FIG. 4.— Absorption coefficients (top panel; the lines marked "+", "−", and "0" correspond to the polarization index $\alpha = +1$, -1, and 0, respectively) and polarizabilities $\chi_{\pm 1}^{\mathrm{H}}$ (middle) and χ_0^{H} (bottom panel) of the partially ionized (solid lines) and fully ionized (dot-dashed lines) plasma for $B = 3 \times 10^{13}$ G, $\rho = 1$ g cm^{-3}, and $T = 3.16 \times 10^5$ K.

θ_B is the angle between $\boldsymbol{B}$ and the z axis, and (see Eqs. [1]–[3]) $\varepsilon' = \varepsilon + \hat{a}$, $\eta' = \eta + \hat{a} + q$. In the usual case where the plasma and vacuum polarizabilities are small ($|\chi_\alpha^{\mathrm{H}}| \ll (4\pi)^{-1}$ and $|\hat{a}|, q, |m| \ll 1$), the polarization parameter β is given by

$$\beta \approx \frac{2\chi_0^{\mathrm{H}} - \chi_{+1}^{\mathrm{H}} - \chi_{-1}^{\mathrm{H}} + (q+m)/(2\pi)}{2\,(\chi_{+1}^{\mathrm{H}} - \chi_{-1}^{\mathrm{H}})} \frac{\sin^2\theta_B}{\cos\theta_B}. \quad (22)$$

The opacity in the mode j can be written as

$$\kappa_j(\omega, \theta_B) = \sum_{\alpha=-1}^{1} |e_\alpha^j(\omega, \theta_B)|^2\, \hat{\kappa}_\alpha(\omega), \quad (23)$$

where $\hat{\kappa}_\alpha$ ($\alpha = -1, 0, 1$) do not depend on θ_B. For a partially ionized, strongly magnetized hydrogen plasma $\hat{\kappa}_\alpha(\omega)$ have been obtained by Potekhin & Chabrier (2003, 2004).

The polarization vectors $\boldsymbol{e}^{\mathrm{X}}$ and $\boldsymbol{e}^{\mathrm{O}}$ for the polarizabilities presented in Figure 3 prove to be indistinguishable from the results for the fully ionized plasma at general θ_B values. They exhibit vacuum polarization resonances at $\hbar\omega \sim 10$ keV related to intersections of χ_{-1}^{H} with the combination of vacuum polarization coefficients $(q+m)/2\pi$ that enters equation (22) (the horizontal dotted line in Fig. 3; in this case $|\chi_0^{\mathrm{H}}|, |\chi_{+1}^{\mathrm{H}}| \ll |\chi_{-1}^{\mathrm{H}}|$) and the electron
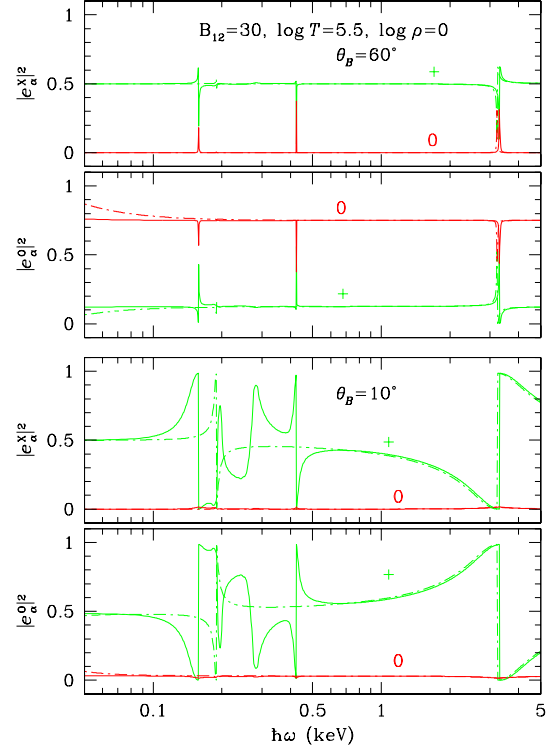

FIG. 5.— Squared moduli of the cyclic components e_α^j of polarization vectors $\boldsymbol{e}^{\mathrm{X}}$ and $\boldsymbol{e}^{\mathrm{O}}$ for the normal waves propagating at angles $\theta_B = 60°$ (two upper panels) and $10°$ (two lower panels) in a hydrogen plasma with $B = 3 \times 10^{13}$ G, $T = 3.16 \times 10^5$ K, $\rho = 1$ g cm^{-3}. Solid lines: partially ionized plasma; dot-dashed lines: full ionization.

cyclotron resonance at $\hbar\omega \approx 27$ keV. If we neglected the CM coupling effect, we would observe additional resonant features near $\hbar\omega = 0.07$ and 0.2 keV, associated with the bound-bound transitions for $\alpha = +1$ (Fig. 2) and $\alpha = 0$ (Fig. 1). Actually these features are smoothed away by the CM coupling.

For the second set of plasma parameters considered in §4, the ionization degree is relatively low ($1 - x_{\mathrm{H}} = 0.11$). Figure 5 shows squared moduli of two components of the polarization vectors, e_0^j and e_{+1}^j (the third component can be found as $|e_{-1}|^2 = 1 - |e_{+1}|^2 - |e_0|^2$) for two propagation angles $\theta_B = 60°$ and $\theta_B = 10°$. Dot-dashed and solid curves correspond to the fully and partially ionized plasma models, respectively. At $\theta_B = 60°$ (two upper panels), there are two sharp resonances for the partially ionized case at $\hbar\omega = 0.158$ and 0.425 keV, associated with the zero level crossings by $\chi_0^{\mathrm{H}}(\omega)$ (the bottom panel of Fig. 4), which are absent in the case of full ionization. The feature at 3.3 keV is the vacuum resonance. At smaller angle (two lower panels of Fig. 5), these resonances become broader, and there appear additionally other features associated with the behavior of χ_{+1}^{H} (see the middle panel of Fig. 4). For the fully ionized plasma, an additional feature is just the proton cyclotron resonance, whereas for the partially ionized case the behavior of the polarization vectors is more complicated because of the influence of the atomic resonances.

Figure 6 shows the opacities calculated according to equation (23), using $|e_\alpha^j|^2$ shown in Figure 5 and $\hat{\kappa}_\alpha(\omega)$
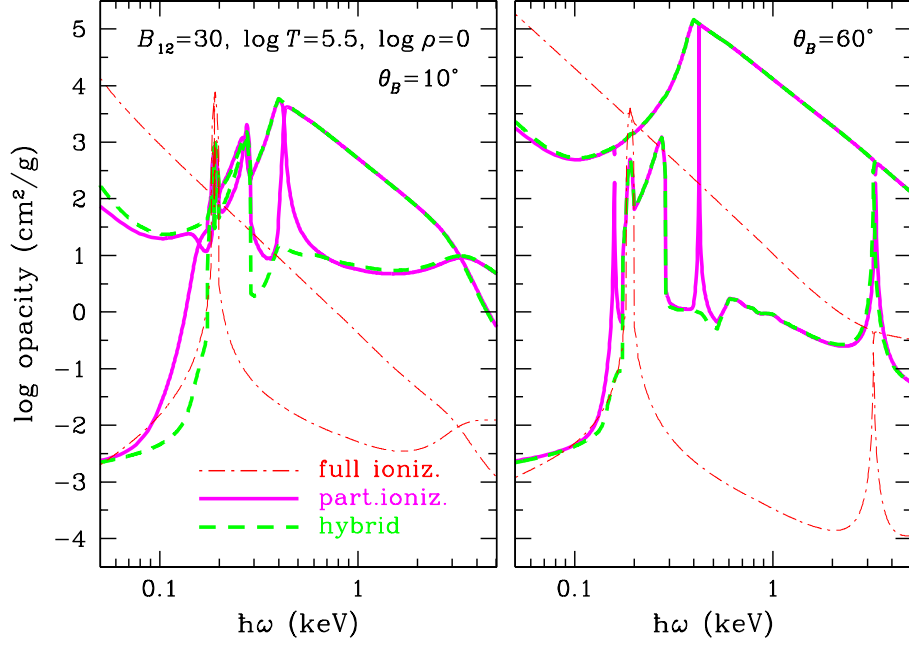
FIG. 6.— Opacities in two modes κ_j (Eq. [23]) for the same plasma parameters as in Fig. 5 and two angles, $\theta_B = 10°$ (left panel) and $\theta_B = 60°$ (right panel). Solid lines: a self-consistent calculation for a partially ionized hydrogen plasma; dashed lines: partially ionized hydrogen plasma within a "hybrid" treatment (a model that uses the basic opacities $\hat{\kappa}_\alpha$ from the model of partially ionized plasma and polarization vectors $\boldsymbol{e}^j$ from the model of full ionization); light dot-dashed lines: model of full ionization. The lower curve of each type is related to extraordinary and the upper one to ordinary mode (the dashed curve often coincides with the solid one).
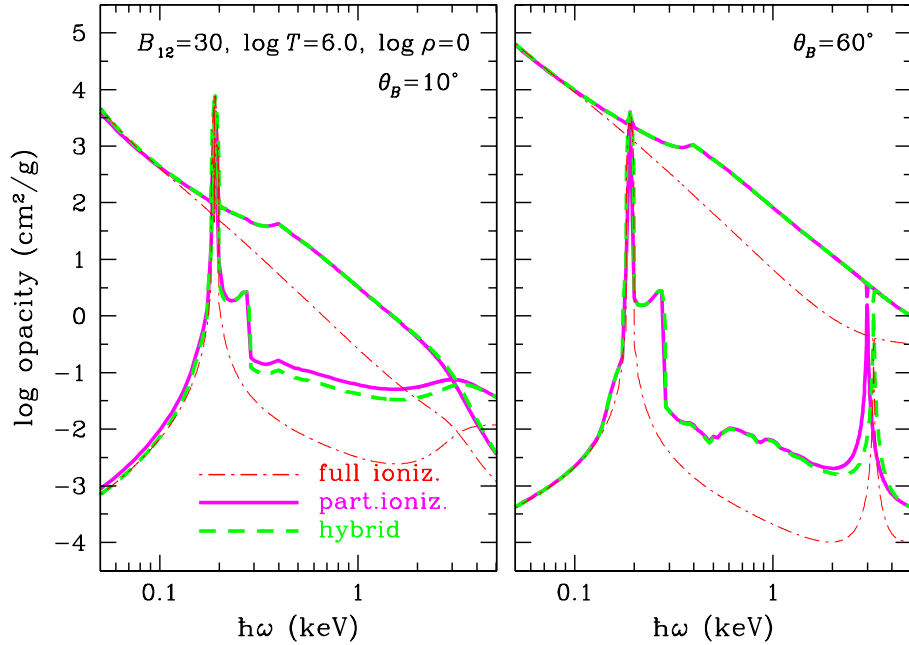
FIG. 7.— Same as in Fig. 6 but for higher temperature, $T = 10^6$ K.

calculated as in Potekhin & Chabrier (2003, 2004). The opacities that take into account partial ionization are plotted by solid lines, and those assuming full ionization by dot-dashed lines. The dashed lines correspond to a hybrid approach, where the polarization of normal modes is described by the formulae for a fully ionized plasma, and $\hat{\kappa}_\alpha(\omega)$ take into account bound-bound and bound-

free atomic transitions (Potekhin & Chabrier 2003). Although this approach is closer to reality than the model of full ionization, there are significant differences from the more accurate result drawn by the solid lines. In particular, the feature near $\hbar\omega = 0.5$ keV is missed in the hybrid approximation.
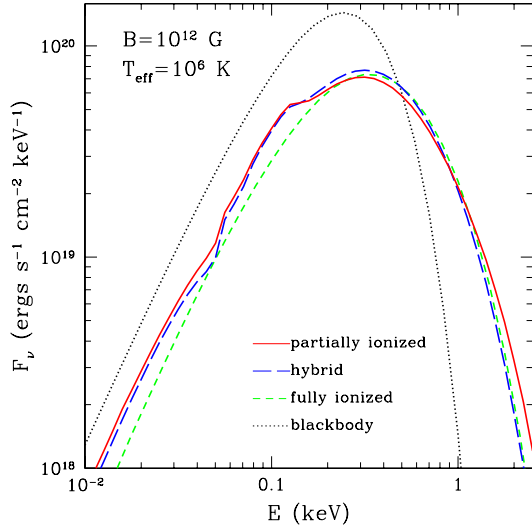
With increasing temperature, the differences between

FIG. 8.— Spectrum of hydrogen atmosphere with $B = 10^{12}$ G (field normal to the surface) and effective temperature $T_{\rm eff} = 10^6$ K. The solid line is for the self-consistent model of a partially ionized atmosphere, the long-dashed line is for the hybrid model, the short-dashed line is for a fully ionized atmosphere, and the dotted line is for a blackbody with $T = T_{\rm eff}$.

the self-consistent and hybrid approximations go away. Figure 7 shows the case where the plasma parameters are the same as in Figure 6, except for $T = 10^6$ K. At this temperature, $x_{\rm H} = 1.4\%$. Such small amount of neutral atoms is still very important for the opacities, but the hybrid approximation yields the result close to self-consistent one.

Summarizing, we conclude that the hybrid approach to calculation of the mode opacities can be applicable if the fraction of bound states in the plasma, $x_{\rm H}$ is small.

6. SPECTRA

Examples of application of the self-consistent opacity calculation for partially ionized hydrogen NS atmospheres are given in Figures 8–10. Here, the atmosphere parameters are the same as for the low-field models in Ho et al. (2003). The solid lines are obtained using the self-consistent calculation of the opacities, while the long-dashed lines reproduce the hybrid treatment described above. The fully ionized plasma model (short dashes) and blackbody (dots) are shown for comparison. The difference in the spectra obtained using the self-consistent and hybrid approaches is partly due to the difference in the temperature profiles within the atmosphere. As expected, this difference is small at relatively low magnetic field $B = 10^{12}$ G and effective temperature $T_{\rm eff} = 10^6$ K (Fig. 8), where the fraction of atoms is small at every optical depth in the atmosphere, but it becomes larger for lower temperature ($T_{\rm eff} = 5 \times 10^5$ K, Fig. 9) or stronger field ($B = 10^{13}$ G, Fig. 10). In the case shown in Figure 9, the temperature profile $T(\rho)$ calculated with the new (self-consistent) opacities is higher by $\sim 10\%$, so that photons come from shallower (lower atomic fraction) layers of the atmosphere, which results in weaker spectral features due to the atomic transitions. A modification of the temperature profile is also responsible for the weaker proton cyclotron feature in this case. At contrast, in the
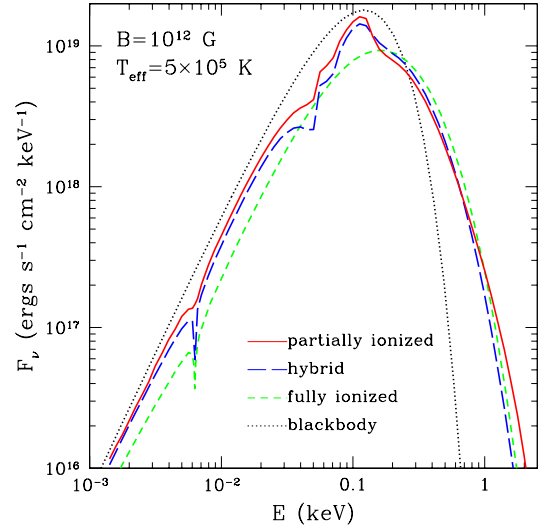

FIG. 9.— Same as in Fig. 8 but for lower effective temperature, $T_{\rm eff} = 5 \times 10^5$ K.

case shown in Figure 10 the temperature profile is lower by $\lesssim 10\%$, and photons come from deeper (higher atomic fraction) layers, resulting in stronger atomic features.

For superstrong fields ($B \gtrsim 10^{14}$ G), the current atmosphere models are less reliable because of the unsolved problems of mode conversion and dense plasma effect (e.g., Ho et al. 2003), whose importance increases with increasing B.

7. CONCLUSIONS AND OUTLOOK

We have studied the polarizability and electromagnetic polarization modes in a partially ionized, strongly magnetized hydrogen plasma. The full account of the coupling of the quantum mechanical structure of the atoms to their center-of-mass motion across the magnetic field is shown to be crucial for the correct evaluation of the polarization properties and opacities of the plasma. The self-consistent treatment of the polarizability and absorption coefficients is ensured by use of the Kramers-Kronig relation. Such treatment proves to be important if the ionization fraction of the plasma is low ($\lesssim 50\%$). For high degree of ionization ($\gtrsim 80\%$), the polarizability of a fully ionized plasma remains a good approximation, just as previously assumed (Potekhin & Chabrier 2003). This approximation was adopted in the NS atmosphere models built in Ho et al. (2003, 2004). A comparison with updated spectra based on the self-consistent treatment (§6) shows that this approximation is satisfactory if $B \lesssim 10^{13}$ G and $T_{\rm eff} \gtrsim 10^6$ K. The self-consistent treatment is needed in the atmospheres of cool or ultramagnetized NSs, with relatively low degrees of ionization.

There are several limitations of the present model, which may become important for the magnetar fields and/or for low $T_{\rm eff}$. While H atoms are treated accurately in our calculations of the EOS and opacities, H_2 molecules are included in the EOS using the static approximation (i.e., without their CM coupling) and neglected in the opacities. Other bound species, such as H_2^+ (e.g., Turbiner & López Vieyra 2003), H_3^{2+} (López Vieyra & Turbiner 2000), and H_n
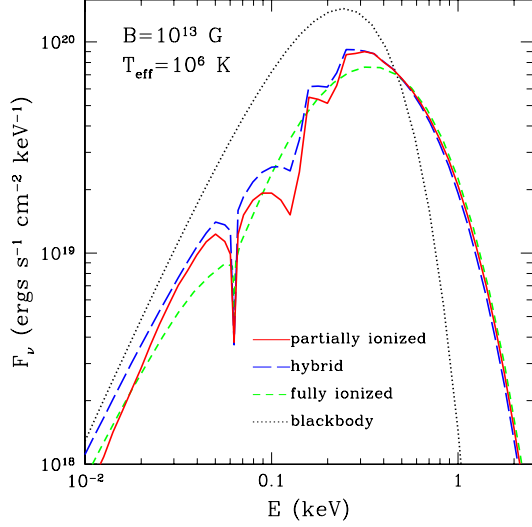
FIG. 10.— Same as in Fig. 8 but for higher field strength, $B = 10^{13}$ G.

slightly higher $T_{\rm eff}$ is needed to ensure negligible abundance of molecules.

Another uncertainty in ultramagnetized NS atmospheres is the dense plasma effect: the decoupling layer for photons in the atmosphere (where optical depth ≈ 1) may occur at high density where the electron plasma frequency exceeds the photon frequency (e.g., Ho et al. 2003; Lloyd 2003). The present treatment is not applicable for such cases. In addition, construction of reliable atmosphere models at $B \gtrsim 10^{14}$ G requires solution of the problem of mode conversion (Lai & Ho 2003a).

Furthermore, for fitting observed spectra one should construct a grid of models with different field orientations and a range of field strengths, and produce angle- and field-integrated synthetic spectra for an assumed field geometry. Since all the discussed spectral resonances are B-dependent, and some of them are θ_B-dependent, we expect that such integration will somewhat smooth the spectral features (Ho & Lai 2004).

chains (Lai, Salpeter, & Shapiro 1992) are not included. Moreover, the NS may have a condensed surface, with negligible vapor above it (Lai & Salpeter 1997; Lai 2001). For a NS with mass $M = 1.4\ M_\odot$ and radius $R = 10$ km, estimates at $\log B$ (G)= 13.5–15 (based on Potekhin & Chabrier 2004) indicate that a thick H atmosphere will be present, and a condensed surface will not occur, provided $T_{\rm eff} \gtrsim 3.8 \times 10^5\,(B/10^{14}\ {\rm G})^{1/4}$ K;

APPENDIX

FITTING FORMULAE FOR THE VACUUM POLARIZATION COEFFICIENTS

The studies of the vacuum polarization by strong fields have long history; an extensive bibliography is given by Schubert (2000). In the low-energy limit, $\hbar\omega \ll m_e c^2$, the Euler-Heisenberg effective Lagrangian can be applied. The relevant dimensionless magnetic-field parameter is $b \equiv B/B_{\rm Q}$, where $B_{\rm Q} = m_e^2 c^3/e\hbar = 4.414 \times 10^{13}$ G. In the limit $b \ll 1$, the vacuum polarization coefficients are given by (Adler 1971)

$$\hat{a} = -\frac{2\alpha_{\rm f}}{45\pi}\,b^2, \quad q = \frac{7\alpha_{\rm f}}{45\pi}\,b^2, \quad m = -\frac{4\alpha_{\rm f}}{45\pi}\,b^2, \tag{A1}$$

where $\alpha_{\rm f} = e^2/\hbar c = 1/137.036$ is the fine-structure constant. For arbitrary B, the tensors of vacuum polarization $\boldsymbol{\chi}^{\rm vac}$ and $\boldsymbol{\mu}$ have been obtained by Heyl & Hernquist (1997) in terms of special functions and by Kohri & Yamada (2002) numerically. The result of Heyl & Hernquist (1997) can be reduced to the following more convenient form:

$$\hat{a} = \frac{\alpha_{\rm f}}{2\pi}\left[\xi X(\xi) - 2\int_1^\xi X(\xi')\,{\rm d}\xi' - 0.0329199\right], \tag{A2}$$

$$\hat{a} + q = \frac{\alpha_{\rm f}}{2\pi}\left[\frac{2}{9\xi^2} - \frac{2}{3}X'(\xi)\right], \tag{A3}$$

$$m = \frac{\alpha_{\rm f}}{2\pi}\left[\xi X(\xi) - \xi^2 X'(\xi)\right], \tag{A4}$$

where $X(\xi)$ is expressed through the Gamma function $\Gamma(x)$:

$$X(\xi) = 2\ln\Gamma(\xi/2) - \frac{1}{3\xi} - \ln\frac{4\pi}{\xi} + \xi + \xi\ln\frac{2}{\xi}, \tag{A5}$$

$$X'(\xi) = {\rm d}X(\xi)/{\rm d}\xi, \qquad \xi = b^{-1}. \tag{A6}$$

Results of calculation according to Eqs. (A2)–(A6) agree with Fig. 2 of Kohri & Yamada (2002) and can be approximately represented by

$$\hat{a} \approx -\frac{2\alpha_{\rm f}}{9\pi}\ln\left(1 + \frac{b^2}{5}\frac{1 + 0.25487\,b^{3/4}}{1 + 0.75\,b^{5/4}}\right), \tag{A7}$$

$$q \approx \frac{7\alpha_{\mathrm{f}}}{45\pi}\, b^2\, \frac{1+1.2\,b}{1+1.33\,b+0.56\,b^2}, \tag{A8}$$

$$m \approx -\frac{\alpha_{\mathrm{f}}}{3\pi}\, \frac{b^2}{3.75+2.7\,b^{5/4}+b^2}. \tag{A9}$$

Equations (A7)–(A9) exactly recover the weak-field limits (A1) and the leading terms in the high-field ($b \gg 1$) expansions (Eqs. [2.15]–[2.17] of Ho & Lai 2003); in the latter regime, Eqs. (A7) and (A8) ensure also the terms next to leading. The maximum errors are 1.1% at $b = 0.07$ for equation (A7), 2.3% at $b = 0.4$ for equation (A8), and 4.2% at $b = 0.3$ for equation (A9).

REFERENCES

Adler, S. L. 1971, Ann. Phys. (N.Y.), 67, 599
Armstrong, B. M., & Nicholls, R. W. 1972, Emission, Absorption and Transfer of Radiation in Heated Atmospheres (Oxford: Pergamon)
Becker, W. & Aschenbach, B. 2002, in 270. WE-Heraeus Seminar on Neutron Stars, Pulsars, and Supernova Remnants, MPE Report 278, ed. W. Becker, H. Lesch, & J. Trümper (Garching: MPE), 64
Bulik, T., & Pavlov, G. G. 1996, ApJ, 469, 373
Ginzburg, V. L. 1970, The Propagation of Electromagnetic Waves in Plasmas, 2nd ed. (London: Pergamon)
Haberl, F. 2004, Adv. Sp. Res., 33, 638
Heyl, J. S., & Hernquist, L. 1997, J. Phys. A, 30, 6485
Ho, W. C. G., & Lai, D. 2001, MNRAS, 327, 1081
Ho, W. C. G., & Lai, D. 2003, MNRAS, 338, 233
Ho, W. C. G., & Lai, D. 2004, ApJ, 607, 420
Ho, W. C. G., Lai, D., Potekhin, A. Y., & Chabrier, G. 2003, ApJ, 599, 1293
Ho, W. C. G., Lai, D., Potekhin, A. Y., & Chabrier, G. 2004, Adv. Sp. Res., 33, 537
Israel, G., Mereghetti, S., & Stella, L. 2002, Mem. Soc. Astron. Ital., 73, 465
Kohri, K., & Yamada, S. 2002, Phys. Rev. D, 65, 043006
Lai, D. 2001, Rev. Mod. Phys., 73, 629
Lai, D., & Ho, W. C. G. 2002, ApJ, 566, 373
Lai, D., & Ho, W. C. G. 2003a, ApJ, 588, 962
Lai, D., & Ho, W. C. G. 2003b, Phys. Rev. Lett. 91, 071101
Lai, D., & Salpeter, E. E. 1997, ApJ, 491, 270
Lai, D., Salpeter, E. E., & Shapiro, S. L. 1992, Phys. Rev. A, 45, 4832
Landau, L. D., & Lifshitz, E. M. 1989, Statistical Physics, Part 1, 3rd Edition (Oxford: Pergamon)
Lloyd, D. A. 2003, MNRAS, submitted [astro-ph/0303561]
López Vieyra, J. C., & Turbiner, A. V. 2000, Phys. Rev. A, 62, 022510

Mészáros, P. 1992, High-Energy Radiation from Magnetized Neutron Stars (Chicago: University of Chicago Press)
Özel, F. 2001, ApJ, 563, 276
Pavlov, G. G., & Mészáros, P. 1993, ApJ, 416, 752
Pavlov, G. G., & Potekhin, A. Y. 1995, ApJ, 450, 883
Pavlov, G. G., & Zavlin, V. E. 2003, in XXI Texas Symposium on Relativistic Astrophysics, ed. R. Bandiera, R. Maiolino, & F. Mannucci (Singapore: World Scientific), 319
Pavlov, G. G., Shibanov, Yu. A., Zavlin, V. E., & Meyer, R. D. 1995, in NATO ASI Ser. C 450, The Lives of the Neutron Stars, ed. M. A. Alpar, Ü. Kiziloğlu, & J. van Paradijs (Dordrecht: Kluwer), 71
Potekhin, A. Y. 1994, J. Phys. B, 27, 1073
Potekhin, A. Y. 1998, J. Phys. B, 31, 49
Potekhin, A. Y., Chabrier G., & Shibanov, Yu. A. 1999, Phys. Rev. E, 60, 2193
Potekhin, A. Y., & Chabrier, G. 2003, ApJ, 585, 955
Potekhin, A. Y., & Chabrier, G. 2004, ApJ, 600, 317
Potekhin, A. Y., & Pavlov, G. G. 1993, ApJ, 407, 330
Potekhin, A. Y., & Pavlov, G. G. 1997, ApJ, 483, 414
Press, W. H., Teukolsky, S. A., Vetterling, W. T., & Flannery, B. P. 1996, Numerical Recipes in Fortran 77: The Art of Scientific Computing (Cambridge: Cambridge University Press)
Schubert, C. 2000, Nucl. Phys. B, 585, 407
Shibanov, Yu. A., & Zavlin, V. E. 1995, Astron. Lett., 21, 3
Shibanov, Yu. A., Pavlov, G. G., Zavlin, V. E., & Ventura, J. 1992, A&A, 266, 313
Turbiner, A. V., & López Vieyra, J. C. 2003, Phys. Rev. A, 68, 012504
Zane, S., Turolla, R., & Treves, A. 2000, ApJ, 537, 387
Zane, S., Turolla, R., Stella, L., & Treves, A. 2001, ApJ, 560, 384